


Magnetic resonance imaging connectivity for the prediction of seizure outcome in temporal lobe epilepsy

*†Victoria L. Morgan , *‡Dario J. Englot, *Baxter P. Rogers, *§Bennett A. Landman, §Ahmet Cakir, ¶Bassel W. Abou-Khalil, and *†Adam W. Anderson

Epilepsia, **(*):1–10, 2017
doi: 10.1111/epi.13762

SUMMARY

Objective: Currently, approximately 60–70% of patients with unilateral temporal lobe epilepsy (TLE) remain seizure-free 3 years after surgery. The goal of this work was to develop a presurgical connectivity-based biomarker to identify those patients who will have an unfavorable seizure outcome 1-year postsurgery.

Methods: Resting-state functional and diffusion-weighted 3T magnetic resonance imaging (MRI) was acquired from 22 unilateral (15 right, 7 left) patients with TLE and 35 healthy controls. A seizure propagation network was identified including ipsilateral (to seizure focus) and contralateral hippocampus, thalamus, and insula, with bilateral midcingulate and precuneus. Between each pair of regions, functional connectivity based on correlations of low frequency functional MRI signals, and structural connectivity based on streamline density of diffusion MRI data were computed and transformed to metrics related to healthy controls of the same age.

Results: A consistent connectivity pattern representing the network expected in patients with seizure-free outcome was identified using eight patients who were seizure-free at 1-year postsurgery. The hypothesis that increased similarity to the model would be associated with better seizure outcome was tested in 14 other patients (Engel class IA, seizure-free: $n = 5$; Engel class IB-II, favorable: $n = 4$; Engel class III–IV, unfavorable: $n = 5$) using two similarity metrics: Pearson correlation and Euclidean distance. The seizure-free connectivity model successfully separated all the patients with unfavorable outcome from the seizure-free and favorable outcome patients ($p = 0.0005$, two-tailed Fisher's exact test) through the combination of the two similarity metrics with 100% accuracy. No other clinical and demographic predictors were successful in this regard.

Significance: This work introduces a methodologic framework to assess individual patients, and demonstrates the ability to use network connectivity as a potential clinical tool for epilepsy surgery outcome prediction after more comprehensive validation.

KEY WORDS: Epilepsy imaging, Functional connectivity, Epilepsy surgery, Resting-state connectivity.



Victoria L. Morgan is an associate professor of radiology and radiological sciences at Vanderbilt University Medical Center.

Temporal lobe epilepsy (TLE) is one of the most common forms of epilepsy and is characterized by seizures originating from a focus in the temporal lobe. Approximately 22%

of these patients fail to respond to antiepileptic drug (AED) treatment.¹ In mesial TLE, it is widely accepted that the hippocampus is the seizure focus, and surgical resection of this

Accepted March 20, 2017.

*Department of Radiology and Radiological Sciences, Vanderbilt University Institute of Imaging Science, Vanderbilt University Medical Center, Nashville, Tennessee, U.S.A.; †Department of Biomedical Engineering, Vanderbilt University, Nashville, Tennessee, U.S.A.; ‡Department of Neurosurgery, Vanderbilt University Medical Center, Nashville, Tennessee, U.S.A.; §Department of Electrical Engineering and Computer Science, Vanderbilt University, Nashville, Tennessee, U.S.A.; and ¶Department of Neurology, Vanderbilt University Medical Center, Nashville, Tennessee, U.S.A.

Address correspondence to Victoria L. Morgan, Department of Radiology and Radiological Sciences, Vanderbilt University Institute of Imaging Science, 1161 21st Avenue South, AA 1105 MCN, Vanderbilt University, Nashville, TN 37232-2310, U.S.A. E-mail: victoria.morgan@vanderbilt.edu

Wiley Periodicals, Inc.

© 2017 International League Against Epilepsy

KEY POINTS

- Approximately 30% of patients with temporal lobe epilepsy continue to have seizures 1 year after surgical treatment
- A consistent functional and structural connectivity model was identified across temporal lobe epilepsy patients with seizure-free outcome
- Similarity to the model predicted surgical outcome at 1 year with 100% accuracy in a small independent test cohort
- If validated, this work demonstrates the potential for the use of connectivity as a clinical tool for prediction of epilepsy surgery outcome

region is a potential, and often preferable, treatment compared to prolonged drug therapy.^{2,3} Currently, however, only approximately 60–70% of patients remain seizure-free 3 years after surgery for unilateral mesial TLE.⁴

There have been many attempts to use standard demographic and clinical variables to identify patients who will benefit most from temporal resection. In TLE with hippocampal sclerosis, factors such as younger age at surgery,⁵ >90% ipsilateral interictal epileptiform discharges,⁶ and less frequent presurgical generalized tonic-clonic seizures (GTCS)⁷ are associated with favorable early seizure outcome. In a cohort of TLE patients including those with and without hippocampal sclerosis, lower presurgical seizure frequency was an indicator of favorable outcome.⁸ Gracia et al.⁹ proposed a composite score in which 75–79% of patients with higher scores (4–6 of 6) had a favorable outcome at 10 years after resection. Points were added to the score for abnormal magnetic resonance imaging (MRI), <20 seizures per month, epilepsy duration <5 years, no GTCS, no invasive recordings, and temporal lobe resection. To predict likelihood of seizure freedom at 2 and 5 years' post-surgery, Jehi et al.¹⁰ developed a nomogram that incorporated the associations between the above-mentioned variables and seizure outcome. In most cases, the greatest chance of seizure freedom predicted by these models is approximately 80%, which is only slightly higher than the success rate of all TLE patients who undergo resection. This suggests that there may be additional factors that help to distinguish which TLE patients will have favorable surgical outcomes, beyond these clinical and demographic variables.

TLE has been associated with altered networks in the brain. MRI provides an efficient method to investigate both the functional (FC) and structural (SC) connectivity of whole brain network alterations in TLE noninvasively. The strength of functional connections can be quantified using correlations of spontaneous low frequency resting functional MRI (fMRI) signal fluctuations.¹¹ In TLE, this has been investigated extensively (see [12] for review). Diffusion-weighted MRI can be used to quantify the local

diffusion in a voxel to estimate the orientation of white matter fiber bundles within it.¹³ Measures such as fractional anisotropy,¹⁴ mean diffusivity,¹⁴ and fiber density¹⁵ have all been used as diffusion-based metrics of structural network connectivity alterations in TLE.

We propose that FC and SC changes in patients with unilateral TLE may predict seizure outcomes more accurately than clinical and demographic variables alone. In this work, we computed a model of the FC and SC within a previously proposed seizure propagation network¹⁶ across a population of unilateral mesial TLE patients with a seizure-free outcome. We then tested the hypothesis that patients with unilateral TLE who have a connectivity pattern similar to this model will have a favorable outcome, whereas those whose pattern differs from this model will have an unfavorable outcome. Our primary goal was to develop a noninvasive, patient-specific method for identifying those patients who have favorable clinical surgical predictors, but who may ultimately have an unfavorable seizure outcome.

MATERIALS AND METHODS

Patient characteristics

Thirty patients with unilateral TLE were recruited for this work. Of those, 22 completed the imaging procedure and had 1-year postsurgical seizure outcomes available (Table 1). Inclusion criteria required standard presurgical evaluation diagnosis of unilateral TLE based on structural imaging with MRI, ictal and interictal electroencephalography (EEG), analysis of seizure semiology, and functional imaging with positron emission tomography (PET). Exclusion criteria included structural abnormalities on MRI other than hippocampal sclerosis. All patients with TLE were scheduled to undergo anterior temporal lobectomy or selective amygdalohippocampectomy, with one patient having hippocampal laser ablation. Seizure outcome was assessed at 1-year postsurgery by an epileptologist using the Engel surgery outcome classification.¹⁷ For association analyses, the seizure outcome was categorized as completely seizure-free (Engel class IA), favorable (Engel class IB–II), or unfavorable (Engel class III–IV). In addition, 35 healthy controls (20 female and 15 male, mean age \pm standard deviation 37.8 ± 12.3 years) with no history of head trauma or neurologic or neuropsychological disease were also enrolled. The control group included at least one control subject who was age (± 3 years) and gender matched to each TLE patient.

Outcome prediction using clinical and demographic characteristics

The outcome for each patient was identified using the three categories as discussed earlier (seizure-free, favorable, and unfavorable). For outcome prediction throughout this work we used two different binary groupings of the three categories. The first separated the patients into completely

Table 1. Patient clinical and demographic information by 1-year postsurgical seizure outcome

		Seizure-free Engel IA (N = 13)	Favorable Engel IB–II (N = 4)	Unfavorable Engel III–IV (N = 5)	Seizure-free and favorable versus unfavorable (p-value)	Seizure-free versus favorable and unfavorable (p-value)
Age (years)	Mean ± SD	40.7 ± 15.3	33.5 ± 10.6	36.0 ± 8.3	0.59*	0.26*
Duration (years)	Mean ± SD	25.6 ± 13.8	16.2 ± 11.8	14.4 ± 17.5	0.12*	0.04*
Age at onset (years)	Mean ± SD	15.1 ± 14.7	24.2 ± 10.0	21.6 ± 12.3	0.70*	0.26*
Frequency GTCS (per month)	Mean ± SD	0.36 ± 1.09	0.02 ± 0.05	0.12 ± 0.17	0.88*	0.55*
Frequency all seizures (per month)	Mean ± SD	8.5 ± 9.1	18.2 ± 30.9	43.9 ± 76.7	0.64*	0.84*
Number of AEDs failed	Mean ± SD	5.3 ± 1.4	5.7 ± 2.8	5.4 ± 1.9	1*	0.94*
Handedness	Left	1	0	2	0.11†	0.54†
	Right	12	4	3		
Side	Left	5	1	1	1†	0.64†
	Right	8	3	4		
History of status	Yes	0	1	0	1†	0.40†
	No	13	3	5		
MTS on MRI	Yes	11	3	3	0.54†	0.60†
	No	2	1	2		
Ictal EEG	Loc	12	3	4	1†	0.54†
	Not Loc	1	1	1		
Interictal EEG	Lat	7	2	4	0.36†	0.67†
	Not Lat	6	2	1		
Invasive recordings	Done	0	0	1	0.22†	0.40†
	Not done	13	4	4		
Interictal PET	Loc	10	2	5	0.29†	1†
	Not Loc	3	2	0		
MTS on pathology	Yes	13	3	3	0.11†	0.05†
	No	0	1	2		
Type of surgery	TL	4	1	2	1†	1†
	SelAH (LA)	9	3	2 (1)		
m-SFS ^a	[0–3]	2	1	2	0.64†	0.60†
	[4–6]	11	3	3		
Epilepsy Surgery Nomogram ^b	Chance of seizure-free	0.64 ± 0.06	0.65 ± 0.10	0.57 ± 0.10	0.12*	0.47*

GTCS, generalized tonic-clonic seizures; AEDs, antiepileptic drugs; status, status epilepticus; MTS, mesial temporal sclerosis; TL, temporal lobectomy; SelAH, selective amygdalohippocampectomy; LA, hippocampal laser ablation; Loc, localized; Lat, lateralized.

*Mann-Whitney (two-tailed) for continuous data.

†Fisher's exact test (two-tailed) for categorical data, $p \leq 0.05$ are in bold and all p-values are uncorrected.

^aModified seizure frequency score computed from [9].

^bChance of complete seizure freedom at 2 years based on¹⁰ nomogram.

Engel seizure outcome score.¹⁷

seizure-free and favorable versus unfavorable, which was meant to identify those with the worst outcome. The second separated patients into completely seizure-free versus favorable and unfavorable, which was meant to identify the seizure-free from those with recurrence of any type. For continuous measures such as age and duration of disease, a nonparametric comparison of means (two-tailed Mann-Whitney) was performed using SPSS version 24 (IBM Corp., Armonk, NY, U.S.A.). For nominal or categorical parameters such as handedness and type of surgery, the Fisher's exact test (two-tailed) was performed using the same software. In addition, the modified seizure freedom score (m-SFS)⁹ and the Epilepsy Surgery Nomogram indicating the chance of seizure freedom at 2 years based on Jehi et al.,¹⁰ both composite scores based on multiple clinical and demographic parameters, were also computed and

compared to the outcome. These analyses allowed outcome associations using MRI connectivity to be compared to existing noninvasive clinical and demographic methods.

Imaging

The imaging was performed using a Philips Achieva 3T MRI scanner (Philips Healthcare, Best, The Netherlands) using a 32-channel head coil. The acquisition included the following: (1) three-dimensional (3D), T1-weighted whole-brain image for intersubject normalization and tissue segmentation (gradient echo, repetition time = 9.1 msec, echo time = 4.6 msec, 192 shots, flip angle = 8 degrees, matrix = 256 × 256, 1 × 1 × 1 mm³), (2) T2*-weighted fMRI blood oxygenation level-dependent image at rest with eyes closed for FC (matrix = 80 × 80, field of view = 240 mm, 34 axial slices, echo time = 35 msec, repetition

time = 2 s, slice thickness = 3.5 mm/0.5 mm gap, 2×300 volumes, 2×10 min), and (3) diffusion-weighted MRI for SC ($b = 1,600$ s/mm², 92 directions, $2.5 \times 2.5 \times 2.5$ mm³, 3 averages). Physiologic monitoring of cardiac and respiratory fluctuations was performed at 500 Hz using the MRI scanner integrated pulse oximeter and the respiratory belt. Informed consent was obtained prior to scanning each subject per Vanderbilt University Institutional Review Board guidelines.

Image processing

We identified a potential seizure propagation network based loosely on the “Network Inhibition Hypothesis” by Yu and Blumenfeld¹⁸ indicating how seizures spread from the temporal lobe to the cortex and cause impaired consciousness. We chose regions well known to be involved in temporal lobe seizures based on imaging and electrophysiologic evidence as referenced below for each region. Finally, we confirmed the involvement of these regions in TLE connectivity through our studies of connectivity and structure and disease characteristics.^{16,19,20} FreeSurfer 5.1 [http://free-surfer.net/] was used to segment the T₁-weighted, 3D image of each subject into its cortical and subcortical gray matter

statistic.²⁸ The FC for the two fMRI series for each subject for each path were then averaged, resulting in an 8×8 nondirectional FC matrix for each subject.

The diffusion-weighted images were processed using FSL software [http://fsl.fmrib.ox.ac.uk/fsl/fslwiki/] probabilistic fiber tracking.¹³ Images were realigned to the b0 image and corrected for eddy current distortions with affine registration. Next, the voxel-wise diffusion parameters were estimated using the Bayesian approach in the BEDPOSTX algorithm. Then the probabilistic fiber-tracking algorithm with crossing fibers (PROBTRACKX) was used to investigate the same network regions utilized in the FC analyses. The process was computed eight times, once for each seed region using the other seven regions as both targets and terminations. Therefore, each time the algorithm computed the trajectories from each voxel in the seed and quantified how many of 5,000 trials reach each target (other seven regions) without passing through the other regions/targets (i.e. direct connections). The tracking was corrected for distance from the seed by weighting the tracking inversely according to distance so that the results are not driven only by local connectivity. The SC value between two regions (A and B) was computed using the equation:

$$SC_{AB} = \left[\frac{\text{tracts } A \rightarrow B}{\text{tot tracts } A \rightarrow \text{all regions}} \times \frac{\text{vox } A}{\text{vox } A + \text{vox } B} \right] + \left[\frac{\text{tracts } B \rightarrow A}{\text{tot tracts } B \rightarrow \text{all regions}} \times \frac{\text{vox } B}{\text{vox } A + \text{vox } B} \right] \quad (1)$$

regions. Then eight regions of interest (ROIs) were identified in each subject including the left and right hippocampus (Hip),²¹ left and right insula (Ins),²² left and right thalamus (Thal),²³ bilateral precuneus (Prec),^{24,25} and bilateral midcingulate (Cing). For the midcingulate region to be consistent with the region identified in the literature,^{19,24} we combined the caudal anterior cingulate and the anterior half of the posterior cingulate. To combine the right and left TLE patients into one cohort, the regions were converted from left and right to ipsilateral (I) and contralateral (C) referring to the side of seizure focus (Fig. 1A,B).

Functional MRI images were preprocessed with SPM8 software [http://www.fil.ion.ucl.ac.uk/spm/software/spm8/] and Matlab (The MathWorks, Inc, Natick, MA, U.S.A.). The following steps were performed: slice timing correction, motion correction, physiologic noise correction using a retrospective image correction (RETROICOR) protocol²⁶ using the pulse oximeter and respiratory belt time series, spatial normalization to the Montreal Neurological Institute template, and spatial smoothing using a $6 \times 6 \times 6$ mm³ full-width, half-maximum (FWHM) Gaussian kernel. Then the normalized fMRI time series were temporally band-pass filtered at 0.0067–0.1 Hz.²⁷ The FC between each pair of regions was computed as the partial Pearson correlation between the average preprocessed fMRI time series in each region, with the average white matter time series and the six motion time series as confounds, converted to a Fisher Z-

where tracts A→B is the number of successful direct streamlines computed between seed region A and target region B with distance correction, tot tracts A→all regions is the total number of streamlines tracked successfully from the seed region A to any of the regions with distance correction, and vox A is the number of voxels in region A. This measure has no units and is a weighted average of the fraction of the streamlines between the two regions with respect to all the streamlines between the regions. This resulted in an 8×8 nondirectional SC matrix for each subject.

The FC and SC values of the controls were linearly fit to age individually for each path. Then each FC and SC of each patient was corrected by subtracting the estimated mean FC or SC of the control of the same age and dividing by the standard deviation yielding FCcorr and SCcorr. The units of both FCcorr and SCcorr are then standard deviations from the average healthy control of the same age, and can be positive or negative indicating increased or decreased connectivity compared to age-matched controls.

A modified degree²⁹ measure for each region of interest was computed using the 8×8 FCcorr and SCcorr matrices for each individual patient. The measure represents the total strength of the connectivity to this region across the entire network. To emphasize the connectivity ipsilateral to the seizure focus over that to midline and contralateral regions, the total connectivity was computed as a weighted linear

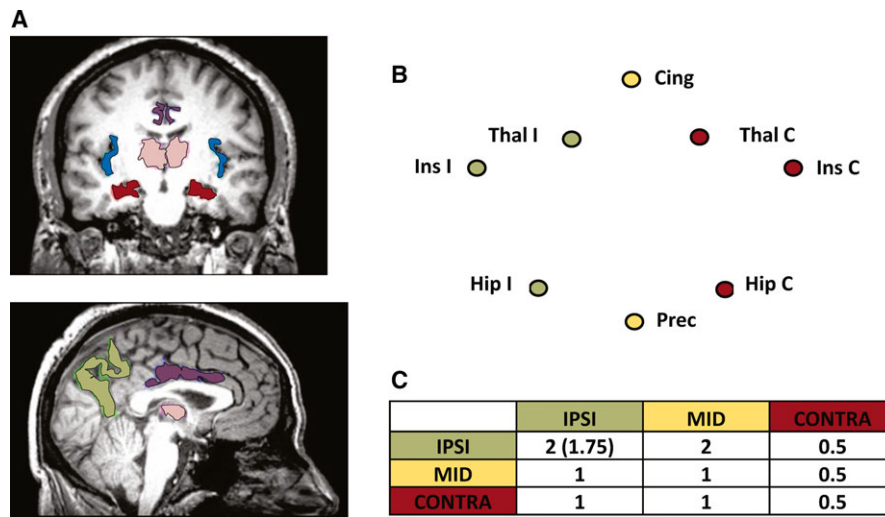


Figure 1.

Seizure propagation network. **(A)** Regions of the network including hippocampus (Hip, red), thalamus (Thal, pink), insula (Ins, blue), mid-cingulate (Cing, purple), and precuneus (Prec, green). **(B)** Network diagram showing the ipsilateral (IPSI, green), midline regions (MID, yellow), and contralateral (CONTRA, red) sets of regions. **(C)** Weights between sets of regions used for weighted connectivity computation. For IPSI to IPSI regions, 2.0 was used for FCcorr calculations, whereas 1.75 was used for SCcorr.

Epilepsia © ILAE

combination of all connectivity values between the region of interest and the other seven regions:

$$\sum_{j=1}^7 (w_{ij} \times \text{CONN}_{ij}) \quad (2)$$

where i is the seed region of interest, and j represents each of the other seven regions of interest in the network (Fig. 1B). The weights, w_{ij} , ranged from 2.0 for ipsilateral to ipsilateral FCcorr connections, to 0.5 for contralateral to contralateral connections as shown in Figure 1C. One value for each region was computed where $\text{CONN}_{ij} = \text{FCcorr}_{ij}$, and one where $\text{CONN}_{ij} = \text{SCcorr}_{ij}$. This resulted in a weighted connectivity vector of 16 values (nodes) (8 regions \times 2 connectivities).

To identify the similarities across the seizure-free patients, the variability in each node was computed across those patients. The FCcorr ipsilateral insula was found to have the highest variability in the seizure-free patients and in all patients (33% increase from next lower variance), and so this node was not used in further analyses. Thus, a 15-node weighted connectivity pattern was used for all subsequent computations. Note that the FCcorr of the ipsilateral insula was still used in the computations of the weighted connectivity of the other nodes.

Creation of connectivity-based model of seizure outcome

The weighted connectivity patterns (15 node vector) from the first 8 of the 13 seizure-free TLE patients enrolled were used to compute the seizure-free connectivity model (training patients). To create the model, we used a resampling and

denoising approach. Principal component analysis³⁰ was performed on six of the eight training patients to reduce the original data into its eigenvectors. Then the six datasets were reconstructed using approximately 80% of the variance using the first three eigenvectors and coefficients, and averaged across the six patients. This process was repeated for all possible combinations of six of the eight training patients, and the resulting connectivity vectors were averaged to produce the seizure-free weighted connectivity model.

Testing of the connectivity-based model of seizure outcome

We hypothesized that the similarity of the individual patient to the model should indicate probability of seizure-free outcome. We identified two parameters of similarity. First, we computed the linear correlation between the patient's connectivity pattern and the model, with higher positive connectivity expected to be associated with seizure freedom. Second, we computed the Euclidean distance between the patient's connectivity pattern and the model, with lower distance expected to be associated with seizure freedom.

To characterize the distribution of possible values for these two similarity measures, we used a Monte Carlo simulation approach where 5,000 new sets of 8×8 FCcorr and SCcorr datasets were simulated. Each one was within 1.5 standard deviations (SD) from the mean of that path. Then a 15-node weighted connectivity vector was computed for each of the 5,000 samples and the similarity metrics to the original model were determined for each. The minimum

correlation of at least 0.1% of the 5,000 sample Monte Carlo data and maximum distance of 99.9% of the Monte Carlo data, were used as thresholds for future patient comparison. The association between binary outcome groups and these similarity thresholds (binary: below or above threshold) were computed using the using the 2×2 Fisher's exact test (two-tailed). Finally, the same procedure was repeated using only the FCcorr data and the SCcorr data individually, to determine whether a model from a single modality performed better than the multimodality model.

RESULTS

The clinical and demographic characteristics of our patient cohort are summarized and stratified by seizure outcome group in Table 1. When seizure-free and favorable outcome patients are compared to unfavorable outcome patients, there are no significant differences between the group and no associations with outcome for any parameter in Table 1. When seizure-free patients are compared to favorable and unfavorable outcome, increased duration of disease ($p = 0.04$, uncorrected) and evidence of mesial temporal sclerosis on pathology ($p = 0.05$, uncorrected) are associated with seizure freedom.

A connectivity-based model of seizure freedom was created using eight seizure-free datasets (Fig. 2A). This model was tested by comparing it to the connectivity patterns of 14

other independent patients using the correlation (Fig. 2B) and Euclidean distance measure (Fig. 2C). A two-dimensional plot of these similarity values for each patient is shown in Figure 3.

The Monte Carlo simulation methodology was used to identify an expected distribution of similarity to the model for seizure-free patients using 5,000 simulated points. The distribution is shown as the gray scale contours in Figure 3. The center of mass of the distribution is [0.6, 8] ([correlation, distance]). The minimum correlation for at least 0.1% of Monte Carlo points is -0.3 , whereas the maximum distance for at least 99.9% of Monte Carlo points is 16. These are shown as dashed lines and were used as cut-off values for the Fisher's exact test statistics.

The seizure-free connectivity model successfully separated all the unfavorable outcome TLE patients (red) from the seizure-free (green) and favorable outcome (yellow) patients ($p = 0.0005$) using the combination of the two similarity measure threshold values (lower right quadrant of Fig. 3) with 100% accuracy. Neither distance to the model alone ($p = 0.02$) (top half of Fig. 3) nor correlation to the model alone (right half of Fig. 3) performed as well at separating the unfavorable patients. Using only functional connectivity (Fig. 4A), the separation was significant ($p = 0.02$) using the distance threshold and both distance and correlation. Using structural connectivity only (Fig. 4B), there was no significant separation between the

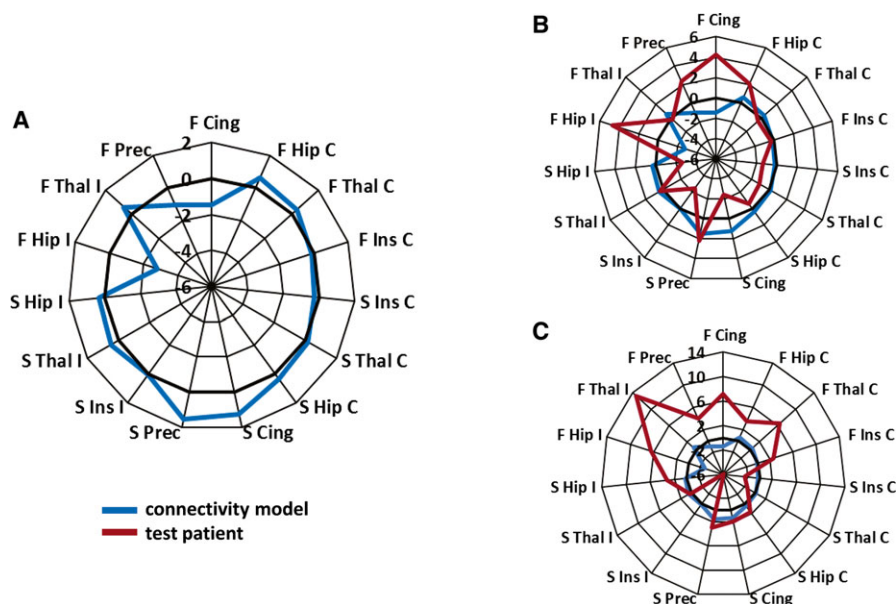


Figure 2.

Functional and structural connectivity model of postsurgical seizure freedom computed from eight seizure-free datasets. (A) Values are weighted connectivity of each node. Nodes are arranged by ipsilateral (left), contralateral (right), FCcorr (top), and SCcorr (bottom). Bold zero line represents value of age-matched healthy control. (B) Model (blue) compared to patient (red, Engel class III) that is highly negatively correlated ($r = -0.60$) with the model. (C) Model (blue) compared to patient (red, Engel III) that has high Euclidean distance (21.4) from the model. Hip, hippocampus; Thal, thalamus; Ins, insula; Prec, precuneus; Cing, midcingulate; I, ipsilateral to seizure onset; C, contralateral to seizure onset; F, FCcorr, functional connectivity corrected for age-matched control; S, SCcorr, structural connectivity corrected for age-matched control.

Epilepsia © ILAE

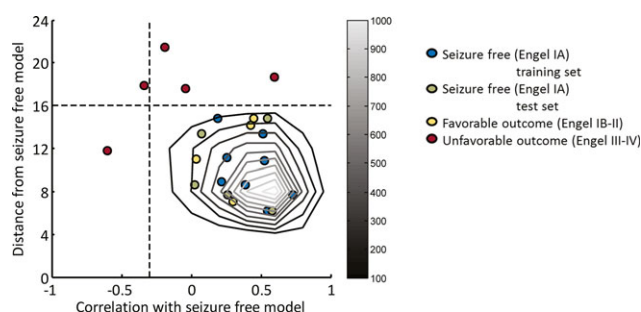


Figure 3.

Testing of connectivity-based model in independent set of patients. Each point represents a single patient. The grayscale contours identify the distribution of similarity measures of 5,000 Monte Carlo simulation points with connectivity of each path in the network within mean ± 1.5 SD of eight seizure-free training patients. The dotted lines indicate the minimum correlation with model of 0.1% of Monte Carlo points at -0.3 , and maximum distance from model of 99.9% of Monte Carlo points at 16. The combination of these two thresholds (lower right quadrant of the plot) correctly separates the unfavorable outcome patients (red) from the favorable (yellow) and seizure-free (green) patients ($p = 0.0005$, two-tailed Fisher's exact test, excluding training set).

Epilepsia © ILAE

patients of different outcomes. The model was not successful in separating the completely seizure-free (green) from the favorable (yellow) and unfavorable (red) outcome TLE patients. Note that the seizure-free training points used in the creation of the model (blue) were not used in these statistical analyses and are shown only for reference.

DISCUSSION

In this preliminary study, we computed a model of presurgical MRI-based functional and structural connectivity, which separated the TLE patients with seizure-free (Engel class IA) and favorable (Engel class IB–II) outcome from those with unfavorable (Engel class III–IV) outcome at 1-year postsurgery with 100% specificity and 100% sensitivity ($p = 0.0005$) in a completely independent test sample of patients (Fig. 3). This model was more accurate than either functional ($p = 0.02$) or structural connectivity alone (Fig. 4). In addition, the connectivity model outperformed several clinical and demographic characteristics in predicting seizure outcome in this cohort (Table 1), as none of these variables could separate the patients with unfavorable outcomes from the others. The model was built on the basic premise that the functional and structural connectivity of the seizure propagation network will have a consistent pattern across those patients with the same presurgical clinical characteristics and a completely seizure-free outcome. It was further hypothesized that those patients with decreased similarity to the model will have worse postsurgical seizure outcome. This premise allows for network heterogeneity in the patients with seizure recurrence, reflecting the fact that clinically it is known that there could be many reasons for TLE surgical failure.³¹

These results suggest that the use of a network connectivity model could have a significant clinical impact on the presurgical evaluation of unilateral TLE. This model can be applied to individual TLE patients as we demonstrated here

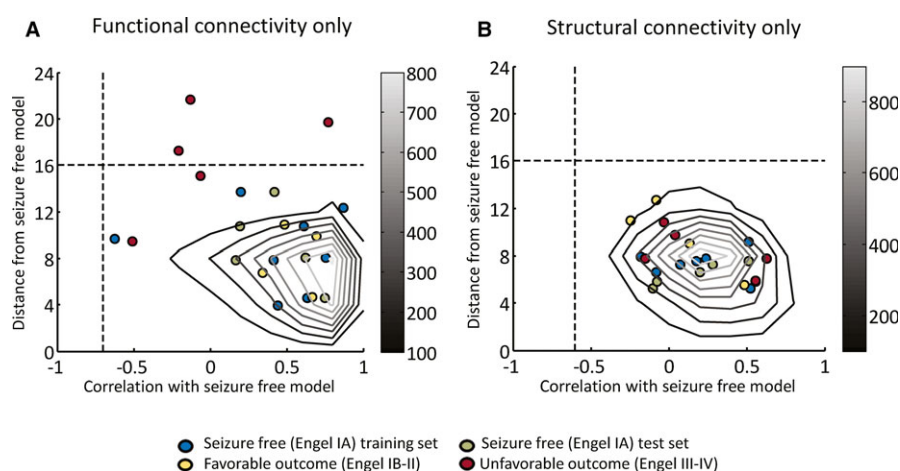


Figure 4.

Testing of functional connectivity-only based model in independent set of patients (A). Testing of structural connectivity-only based model in independent set of patients (B). Each point represents a single patient. The grayscale contours identify the distribution of similarity measures of 5,000 Monte Carlo simulation points with connectivity of each path in the network within mean ± 1.5 SD of eight seizure-free training patients. The vertical dotted lines indicate the minimum correlation with model of 0.1% of Monte Carlo points at -0.7 and -0.6 in (A) and (B), respectively. The horizontal dotted lines indicate the maximum distance from model of 99.9% of Monte Carlo points at 16 in both (A) and (B), respectively. The distance threshold and the combination of these two thresholds (lower right quadrant of the plot) correctly separates the unfavorable patients from the others ($p = 0.02$, two-tailed Fisher's exact test, excluding training set) in functional connectivity model only (A). There is no significant separation of outcomes using structural connectivity alone (B).

Epilepsia © ILAE

by testing it in 14 independent patients (not included in model development) across three different surgical outcome categories. If validated in a larger cohort, it may be possible to add this assessment to the clinical presurgical pipeline to evaluate those patients with unilateral TLE who indicate a good chance of seizure freedom (i.e., those with high m-SFS⁹ and Epilepsy Surgery Nomogram¹⁰ values). Ultimately, it may be possible that the type and nodes of difference from the model may provide some targets of further investigation of the patient such as invasive monitoring, but this has not been explored in this cohort.

Others have used imaging-based connectivity as a biomarker of surgical outcome in TLE. One such report found that increased ipsilateral FC to the resected region was associated with increased chance of seizure freedom ($p < 0.05$).³² Similarly, increased magnetoencephalography connectivity to the resected region was also associated with increased chance of seizure freedom.³³ However, these methods are not currently applicable to individual patients. Bonilha et al.³⁴ used fewer paths across the brain with abnormal SC compared to controls as an indicator of increased chance of seizure freedom. Including clinical variables with the SC, the model achieved 94% specificity and 88% accuracy using a k-fold cross-validation approach.

Our results suggested that functional connectivity alone was partially able to separate the patients with unfavorable outcomes from the others, but the model patients (Fig. 4A, blue) that fell outside the simulation results indicates high variability in FCcorr across even those with seizure-free outcome. The fact that no patients fell outside the seizure-free simulations using only structural data (Fig. 4B) suggests that there was relatively little variability in SCcorr across all patients in this network. It is possible, however, that there are structural abnormalities outside the investigated network that might provide better differentiation between outcomes. Alternatively, the model itself can provide insight into the relationship between the connectivity in the patients (seizure-free) and healthy controls.

In this work, the model (Fig. 2A) showed decreased (<0) FCcorr in the ipsilateral hippocampus and in the bilateral midline structures (precuneus and midcingulate) compared to controls. Increases (>0) in FCcorr were found in the ipsilateral thalamus, the contralateral hippocampus, and contralateral thalamus. Almost all reports of FC changes in TLE detect both increases and decreases throughout the brain with inconsistencies regarding relation to ipsilateral versus contralateral networks.¹² Some report decreased ipsilateral FC with increased contralateral FC,³⁵ similar to our findings, whereas others report mixed or increased ipsilateral FC.^{36,37} These inconsistencies may be due in part to differences in duration of disease, age of subjects, or heterogeneity in surgical outcome.

The seizure-free model showed increased (>0) SCcorr in the bilateral midline structures (precuneus and

midcingulate) compared to controls. Most fiber-tracking literature of TLE reports decreased SC as measured by fractional anisotropy and increased mean diffusivity in TLE.³⁸ When utilizing streamline or fiber density as a measure of SC, a measure similar to ours, both decreases¹⁵ and increases have been reported.³⁹ The measure of streamline density is thought to reflect the “trackability” of the connection from the seed to the target via its most likely principal diffusion direction.¹³ This is affected by parameters such as crossing fibers, myelination, and axon integrity.⁴⁰ Our results imply that decreased FCcorr accompanied by increased SCcorr in midline structures may be caused by or facilitate seizure propagation from the temporal lobe to the cortex.

One novel aspect of this work is the normalization of the connectivity to age. Although this makes it possible to interpret the values more easily within and between subjects and measures, it assumes a linear relationship between these parameters. Early age at onset epilepsy can have many other consequences that are not captured in a linear relationship. Further investigation into this is required. Other limitations of this work are that patients undergoing three types of surgical intervention were considered together, and the follow-up of 1 year is relatively short.

The primary limitation of this study is the small sample size. However, we propose that the promising results of this pilot study warrant further investigation. This work included all patients in our institution who were considered “pure” mesial temporal epilepsy surgical candidates over a 4-year period and a 1-year follow-up who agreed to participate (about 80% of total patients meeting criteria). As described in Table 1, the patients included those with and without hippocampal abnormalities on presurgical MRI in each outcome group, a reflection of our total clinical cohort. As such there is no evidence that the model separated patients based on this parameter. In addition, the two patients with normal hippocampal presurgical MRI with seizure-free outcome were among the first eight patients recruited and were, therefore, included in the training data for computation of the model of seizure-free outcome. Histopathologic evaluation showed that all seizure-free patients had evidence of mesial temporal abnormalities. Those without presurgical MRI evidence of hippocampal abnormality in the favorable and unfavorable outcome groups had hippocampal reactive gliosis (all three patients) and amygdala grade 1 ganglioma (Engel class IV) on pathologic evaluation, but were successfully distinguished based on outcome and not on pathology by our model (Appendix S1).

CONCLUSIONS

In this preliminary work, we developed an MRI functional and structural connectivity model that identified those TLE patients with unfavorable seizure outcome at 1-year

postsurgery with 100% accuracy in this small cohort in which no other clinical and demographic predictors were successful in this regard. The model is unique in that it employs a widespread network with relatively few nodes to specifically seizure propagation. Therefore, this work introduces a methodologic framework to assess individual patients, and demonstrates the ability to use network connectivity as a potential clinical tool for epilepsy surgery outcome prediction. Future work requires validation in a larger patient population and quantification of variability related to scanners and imaging acquisition parameters.

ACKNOWLEDGMENTS

This work was supported by National Institutes of Health (NIH) R01 NS075270 (VLM). We are grateful to the Vanderbilt University multidisciplinary epilepsy clinical care team and their patients for their participation in this research.

DISCLOSURE

None of the authors has any conflict of interest to disclose. We confirm that we have read the Journal's position on issues involved in ethical publication and affirm that this report is consistent with those guidelines.

REFERENCES

1. Laxer KD, Trinka E, Hirsch LJ, et al. The consequences of refractory epilepsy and its treatment. *Epilepsy Behav* 2014;37:59–70.
2. Langfitt JT, Wiebe S. Early surgical treatment for epilepsy. *Curr Opin Neurol* 2008;21:179–183.
3. Wiebe S, Blume WT, Girvin JP, et al. A randomized, controlled trial of surgery for temporal-lobe epilepsy. *N Engl J Med* 2001;345:311–318.
4. Janszky J, Janszky I, Schulz R, et al. Temporal lobe epilepsy with hippocampal sclerosis: predictors for long-term surgical outcome. *Brain* 2005;128:395–404.
5. Ozkara C, Uzan M, Benbir G, et al. Surgical outcome of patients with mesial temporal lobe epilepsy related to hippocampal sclerosis. *Epilepsia* 2008;49:696–699.
6. Paglioli E, Palmini A, Paglioli E, et al. Survival analysis of the surgical outcome of temporal lobe epilepsy due to hippocampal sclerosis. *Epilepsia* 2004;45:1383–1391.
7. Asadi-Pooya AA, Nei M, Sharan A, et al. Historical risk factors associated with seizure outcome after surgery for drug-resistant mesial temporal lobe epilepsy. *World Neurosurg* 2016;89:78–83.
8. Foldvary N, Nashold BE, Mascha E, et al. Seizure outcome after temporal lobectomy for temporal lobe epilepsy – A Kaplan-Meier survival analysis. *Neurology* 2000;54:630–634.
9. Gracia CG, Yardi R, Kattan MW, et al. Seizure freedom score: a new simple method to predict success of epilepsy surgery. *Epilepsia* 2015;56:359–365.
10. Jehi L, Yardi R, Chagin K, et al. Development and validation of nomograms to provide individualised predictions of seizure outcomes after epilepsy surgery: a retrospective analysis. *Lancet Neurol* 2015;14:283–290.
11. Biswal B, Yetkin FZ, Haughton VM, et al. Functional connectivity in the motor cortex of resting human brain using echo-planar MRI. *Magn Reson Med* 1995;34:537–541.
12. Englot DJ, Konrad PE, Morgan VL. Regional and global connectivity disturbances in focal epilepsy, related neurocognitive sequelae, and potential mechanistic underpinnings. *Epilepsia* 2016;57:1546–1557.
13. Behrens TE, Berg HJ, Jbabdi S, et al. Probabilistic diffusion tractography with multiple fibre orientations: what can we gain? *NeuroImage* 2007;34:144–155.
14. Focke NK, Yogarajah M, Bonelli SB, et al. Voxel-based diffusion tensor imaging in patients with mesial temporal lobe epilepsy and hippocampal sclerosis. *NeuroImage* 2008;40:728–737.
15. Bonilha L, Nesland T, Martz GU, et al. Medial temporal lobe epilepsy is associated with neuronal fibre loss and paradoxical increase in structural connectivity of limbic structures. *J Neurol Neurosurg Psychiatry* 2012;83:903–909.
16. Morgan VL, Abou-Khalil B, Rogers BP. Evolution of functional connectivity of brain networks and their dynamic interaction in temporal lobe epilepsy. *Brain Connect* 2015;5:45–59.
17. Engel J, Van Ness PC, Rasmussen TB, et al. Outcome with respect to epileptic seizures. In Engel J (Ed) *Surgical Treatment of the Epilepsies*. New York: Raven Press; 1993:609–621.
18. Yu L, Blumenfeld H. Theories of impaired consciousness in epilepsy. *Disorders of Consciousness. Ann N Y Acad Sci* 2009;1157:48–60.
19. Holmes MJ, Yang X, Landman BA, et al. Functional networks in temporal-lobe epilepsy: a voxel-wise study of resting-state functional connectivity and gray-matter concentration. *Brain Connect* 2013;3:22–30.
20. Morgan VL, Conrad BN, Abou-Khalil B, et al. Increasing structural atrophy and functional isolation of the temporal lobe with duration of disease in temporal lobe epilepsy. *Epilepsy Res* 2015;110:171–178.
21. Malmgren K, Thom M. Hippocampal sclerosis Origins and imaging. *Epilepsia* 2012;53:19–33.
22. Blauwblomme T, David O, Minotti L, et al. Prognostic value of insular lobe involvement in temporal lobe epilepsy: a stereoelectroencephalographic study. *Epilepsia* 2013;54:1658–1667.
23. Blumenfeld H, Varghese GI, Purcaro MJ, et al. Cortical and subcortical networks in human secondarily generalized tonic-clonic seizures. *Brain* 2009;132:999–1012.
24. Fahoum F, Lopes R, Pittau F, et al. Widespread epileptic networks in focal epilepsies: EEG-fMRI study. *Epilepsia* 2012;53:1618–1627.
25. Haneef Z, Lenartowicz A, Yeh HJ, et al. Functional connectivity of hippocampal networks in temporal lobe epilepsy. *Epilepsia* 2014;55:137–145.
26. Glover GH, Li TQ, Ress D. Image-based method for retrospective correction of physiological motion effects in fMRI: RETROICOR. *Magn Reson Med* 2000;44:162–167.
27. Cordes D, Haughton VM, Arfanakis K, et al. Frequencies contributing to functional connectivity in the cerebral cortex in “resting-state” data. *AJNR Am J Neuroradiol* 2001;22:1326–1333.
28. Fisher RA. Frequency distribution of the values of the correlation coefficient in samples from an indefinitely large population. *Biometrika* 1915;10:507–521.
29. Rubinov M, Sporns O. Complex network measures of brain connectivity: uses and interpretations. *NeuroImage* 2010;52:1059–1069.
30. Jolliffe IT. *Principal Component Analysis*, 2nd Ed. Springer Series in Statistics. Berlin-Heidelberg: Springer; 2002.
31. Ramos E, Benbadis S, Vale FL. Failure of temporal lobe resection for epilepsy in patients with mesial temporal sclerosis: results and treatment options Clinical article. *J Neurosurg* 2009;110:1127–1134.
32. Negishi M, Martuzzi R, Novotny EJ, et al. Functional MRI connectivity as a predictor of the surgical outcome of epilepsy. *Epilepsia* 2011;52:1733–1740.
33. Englot DJ, Hinkley LB, Kort NS, et al. Global and regional functional connectivity maps of neural oscillations in focal epilepsy. *Brain* 2015;138:2249–2262.
34. Bonilha L, Jensen JH, Baker N, et al. The brain connectome as a personalized biomarker of seizure outcomes after temporal lobectomy. *Neurology* 2015;84:1846–1853.
35. Pereira FRS, Alessio A, Sercheli MS, et al. Asymmetrical hippocampal connectivity in mesial temporal lobe epilepsy: evidence from resting state fMRI. *BMC Neurosci* 2010;11:66.
36. Liao W, Zhang ZQ, Pan ZY, et al. Altered functional connectivity and small-world in mesial temporal lobe epilepsy. *PLoS One* 2010;5:e8525.
37. Maccotta L, He BJ, Snyder AZ, et al. Impaired and facilitated functional networks in temporal lobe epilepsy. *Neuroimage Clin* 2013;2:862–872.

38. Besson P, Dinkelacker V, Valabregue R, et al. Structural connectivity differences in left and right temporal lobe epilepsy. *NeuroImage* 2014;100:135–144.
39. Dinkelacker V, Valabregue R, Thivard L, et al. Hippocampal-thalamic wiring in medial temporal lobe epilepsy: enhanced connectivity per hippocampal voxel. *Epilepsia* 2015;56:1217–1226.
40. Jones DK, Knosche TR, Turner R. White matter integrity, fiber count, and other fallacies: the do's and don'ts of diffusion MRI. *NeuroImage* 2013;73:239–254.

SUPPORTING INFORMATION

Additional Supporting Information may be found in the online version of this article:

Appendix S1. Supplementary material.